

Optimal Power Flow for Integrated Primary-Secondary Distribution Networks with Center-Tapped Service Transformers

Rui Cheng, *Member, IEEE*, Naihao Shi, *Student Member, IEEE*, Zhaoyu Wang, *Senior Member, IEEE*, Zixiao Ma, *Member, IEEE*

Abstract—Secondary distribution networks (SDNets) play an increasingly important role in smart grids due to a high proliferation of distributed energy resources (DERs) in SDNets. However, most existing optimal power flow (OPF) problems do not take into account SDNets with center-tapped service transformers. Handling the nonlinear and nonconvex SDNet power flow constraints is still an outstanding problem. To meet this gap, we first utilize the second-order cone programming relaxation and linearization to make center-tapped service transformer constraints convex, respectively. Then, a linearized triplex service line power flow model, including its compact matrix-vector form, is further developed to compose the SDNet OPF model with our proposed center-tapped service transformer model. This proposed SDNet OPF model can be easily embedded into existing primary distribution network (PDNet) OPF models, resulting in a holistic power system decision-making solution for integrated primary-secondary distribution networks. Case studies are presented for two different integrated primary-secondary distribution networks that demonstrate the effectiveness and superiority of this model.

Index Terms—Secondary distribution network, center-tapped service transformer, integrated primary-secondary distribution networks, optimal power flow (OPF).

I. INTRODUCTION

Optimal power flow (OPF) is a powerful tool that is widely used in the operation and planning of power systems to optimize economic, reliability, and environmental objectives. Nowadays, OPF at the distribution network level is increasingly compelling due to the high penetration of distributed energy resources (DERs) in distribution networks. One of the biggest challenges for OPF at the distribution network level is the nonlinear power flow equations make OPF non-convex, hindering the high-efficiency computation and calculation. The convex relaxation and linearization for OPF at the distribution network level have been widely studied and investigated in recent decades.

Most studies on the convex relaxation and linearization for OPF at the distribution network level are for primary distribution networks (PDNets), which are typically medium-voltage networks. It can be further classified into two categories: (1) single-phase PDNet OPF; (2) multi-phase unbalanced PDNet OPF.

For single-phase PDNets, second-order cone programming (SOCP) relaxations [1]-[2], semidefinite (SDP) relaxations [3]-[4], and chordal relaxations [5]-[6] are explored to convex-

ify its OPF problems. The linearization of non-linear single-phase power flow, based on the bus injection model, is proposed in [7]. The classical linearized distribution flow (*LinDistFlow*) [8]-[9], based on the branch flow model, is developed by neglecting the non-linear power loss term. Moreover, the compact representation of *LinDistFlow* is proposed in [10]-[11] by means of graph-based matrices. However, those works on PDNet OPF cannot be applied to the real-world multi-phase distribution networks. To increase empirical fidelity, researchers and engineers strive to explore the convex relaxation and linearization for multi-phase PDNet OPF. SDP relaxations are proposed for unbalanced microgrids in [12] and radial unbalanced PDNets in [13], respectively. The *LinDistFlow* model is further extended to multi-phase unbalanced PDNets in [13]-[15]. Some advanced online linearization methods are studied to make the unbalanced PDNet power flow linear. For example, an online feedback-based linearized power flow model for unbalanced PDNets [16] is studied by leveraging the instantaneous voltage and load measurements to update its parameters in real time. In addition, some researchers in [17]-[19] consider transformers in the PDNet OPF by simply expressing and including them as the PDNet admittance matrix.

However, all these works focus on single-phase and multi-phase PDNets without considering low-voltage secondary distribution networks (SDNets). Meanwhile, recent years have witnessed the increasing proliferation of loads and DERs connected to SDNets. In previous distribution network OPF works, loads and DERs in SDNets are aggregated at the PDNet bus, neglecting the power flow in *SDNets with service transformers*. In U.S., loads and DERs in SDNets are connected to the PDNet via center-tapped service transformers. Such an aggregation could introduce errors in the comprehensive distribution network analysis, lacking empirical fidelity. Without explicitly considering SDNets in OPF, the SDNet operating status cannot be accurately estimated. For instance, those works cannot detect and analyze over- and under-voltage problems in SDNets. Moreover, with the increasing proliferation of grid-edge resources, managing the voltage quality in SDNets is more challenging.

Therefore, considering SDNet power flow in OPF is extremely vital for performing trustworthy, reliable, and practical distribution network analysis. There have been several works considering SDNets in distribution networks. The works [20], [21] demonstrate service transformer and triplex service line modeling in SDNets. The article [22] surveys various technical

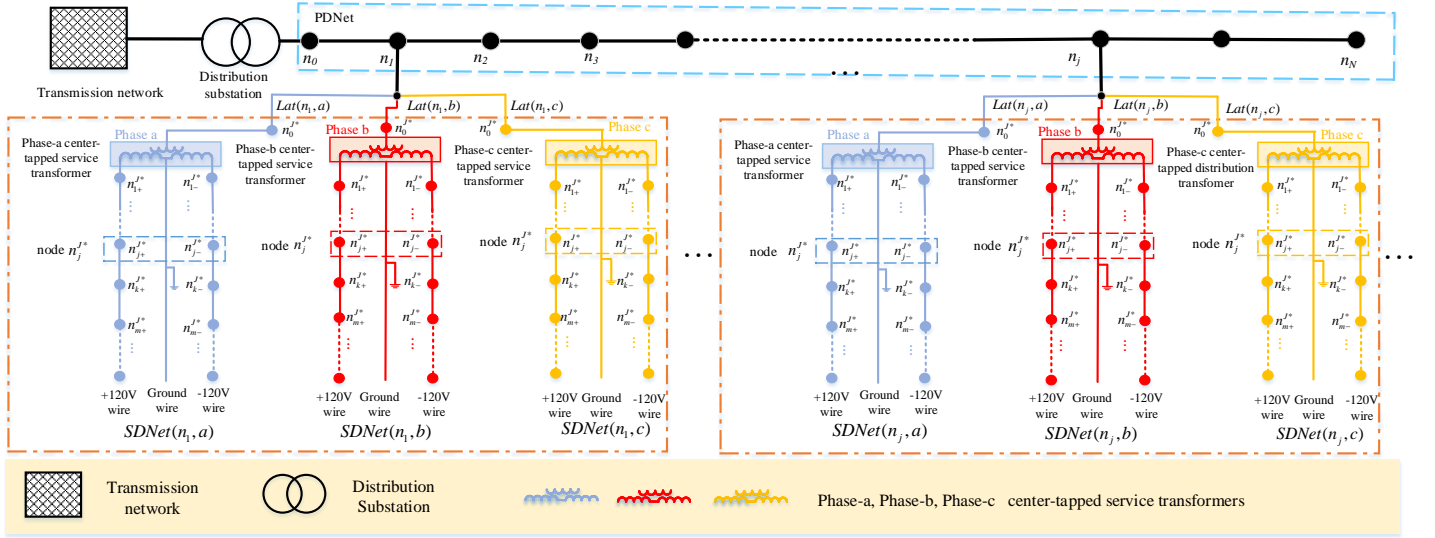


Fig. 1. Integrated Primary-Secondary Distribution Network Illustration

requirements for integration of the roof-top PV into the existing low voltage distribution network. In [23], researchers propose a hierarchical multilevel optimal power flow to minimize power losses in integrated primary-secondary distribution networks. But it does not provide a comprehensive treatment of the power flow in SDNets with service transformers. The work [24] proposes distributed optimal conservation voltage reduction for integrated primary-secondary distribution networks. However, this work simply regards a SDNet as a prosumer without considering service line segment and service transformer modeling, as well as power flow constraints. Service transformer and triplex service line power flow constraints in SDNets are non-linear and non-convex, resulting in challenges and difficulties in OPF solutions. The problem of incorporating service transformers and triplex service lines in SDNets into generalized OPF problems remains unresolved.

To meet this gap, we propose an integrated primary-secondary distribution network OPF model, where service transformers and triplex service lines at the SDNet are carefully considered. This OPF model enables considering distributed energy resources at both the primary and secondary distribution networks, thus bridging the gap between the PDNet optimization and SDNet optimization with increasing empirical fidelity. Compared with existing studies, the main contributions of this study are as follows:

- A generalized integrated primary-secondary distribution network OPF is proposed. This OPF model carefully takes into account service transformer and triplex service lines, leading to a holistic power system decision-making solution at the distribution system level.
- To resolve the nonlinear power flow constraints for service transformers, SOCP relaxation and linearization are applied to make service transformer constraints convex, respectively.
- Linearized power flow model is proposed for triplex service lines in the SDNet. In addition, its compact matrix-

vector form is further developed by utilizing the graph structure of SDNet. Numerical studies show it provides a good estimate of real SDNet power flows by comparing its results with the nonlinear SDNet power flow.

II. PRIMARY DISTRIBUTION NETWORK MODEL

The PDNet is an unbalanced radial primary distribution network PDNet. Let $\{n_0\} \cup \mathcal{N}$ denote the bus index set, where 0 is the index for the head bus and $\mathcal{N} = \{n_1, n_2, \dots, n_N\}$ is the index set for all non-head buses. For each bus $n_I \in \mathcal{N}$, let $\Phi_I \subseteq \{a, b, c\}$ denote the phase set of bus n_I . Let $v_I^{\phi_I}$, $p_I^{\phi_I}$ and $q_I^{\phi_I}$ denote the phase- ϕ_I squared voltage magnitude, real and reactive power loads at bus n_I in the PDNet, where $\phi_I \in \Phi_I$. And let $\mathbf{v}_I = [v_I^{\phi_I}]_{\phi_I \in \Phi_I}$, $\mathbf{p}_I = [p_I^{\phi_I}]_{\phi_I \in \Phi_I}$, $\mathbf{q}_I = [q_I^{\phi_I}]_{\phi_I \in \Phi_I}$. Let \mathcal{L} denote the PDNet edge set. For each line segment $(n_I, n_J) \in \mathcal{L}$, let \mathbf{P}_{IJ} , \mathbf{Q}_{IJ} denote the real and reactive power flow vectors over the line segment (n_I, n_J) in the PDNet, and let $\mathbf{Z}_{IJ} = \mathbf{R}_{IJ} + j\mathbf{X}_{IJ}$ denote the impedance matrix of line segment (n_I, n_J) in the PDNet, including the self-impedance and mutual impedances of phases. For any line segment (n_I, n_J) in the PDNet, the linearized PDNet power flow [13] can be expressed as follows:

$$\mathbf{P}_{IJ} = \sum_{(n_J, n_K) \in \mathcal{L}} \mathbf{P}_{JK} + \mathbf{p}_J \quad (1a)$$

$$\mathbf{Q}_{IJ} = \sum_{(n_J, n_K) \in \mathcal{L}} \mathbf{Q}_{JK} + \mathbf{q}_J \quad (1b)$$

$$\mathbf{v}_I = \mathbf{v}_J + 2[\bar{\mathbf{R}}_{IJ}\mathbf{P}_{IJ} + \bar{\mathbf{X}}_{IJ}\mathbf{Q}_{IJ}] \quad (1c)$$

where

$$\mathbf{a} = [1, e^{-j2\pi/3}, e^{j2\pi/3}]^T, \quad \mathbf{a}^H = \text{conjugate transpose of } \mathbf{a}$$

$$\bar{\mathbf{R}}_{ij} = \text{real}(\mathbf{a}\mathbf{a}^H) \odot \mathbf{R}_{ij} + \text{imag}(\mathbf{a}\mathbf{a}^H) \odot \mathbf{X}_{ij}$$

$$\bar{\mathbf{X}}_{ij} = \text{real}(\mathbf{a}\mathbf{a}^H) \odot \mathbf{X}_{ij} - \text{imag}(\mathbf{a}\mathbf{a}^H) \odot \mathbf{R}_{ij}$$

\odot = element-wise multiplication operator

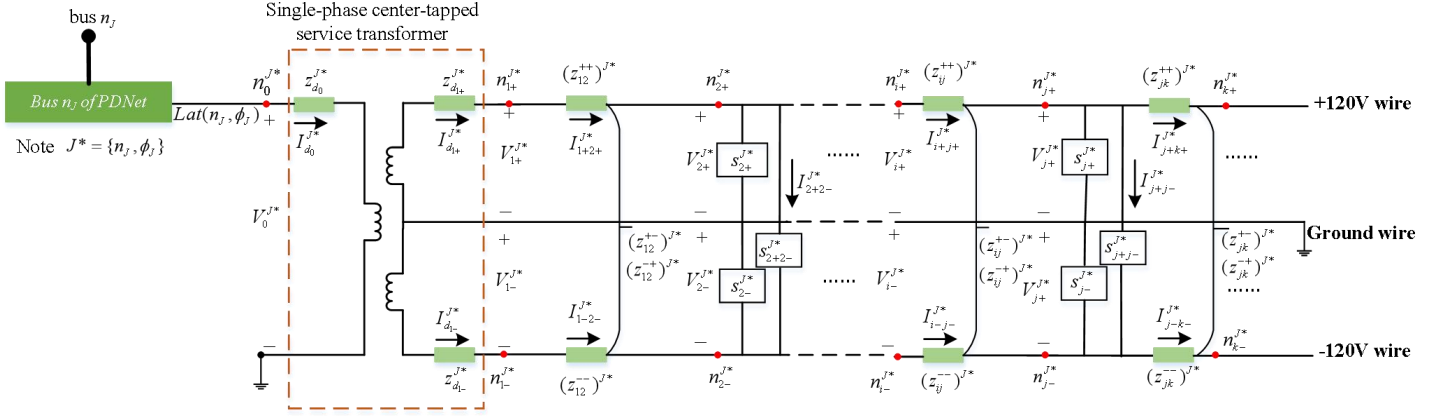


Fig. 2. The secondary distribution network $SDNet(n_J, \phi_J)$, connected to bus n_J of PDNet by a phase- ϕ_J lateral line $Lat(n_J, \phi_J)$.

III. SECONDARY DISTRIBUTION NETWORK MODEL

A. Overview

This section mainly introduces the SDNet model, consisting of center-tapped service transformers and triplex service lines, and its nonlinear power flow.

B. Radial Secondary Distribution Network

Hereafter, for ease of notation, we set $J^* = \{n_J, \phi_J\}$, for any variable $(\cdot)^{J^*}$ with superscript J^* , this superscript J^* indicates the SDNet, $(\cdot)^{J^*}$ belongs to, is $SDNet(n_J, \phi_J)$. With respect to $SDNet(n_J, \phi_J)$, the head-node $n_0^{J^*}$ of $SDNet(n_J, \phi_J)$ is electrically connected to bus n_J of PDNet by a phase- ϕ_J lateral line $Lat(n_J, \phi_J)$ and that includes a single-phase- ϕ_J center-tapped service transformer. An integrated primary-secondary distribution network illustration is shown in Fig.1.

The center-tapped service transformer consists of three windings. As shown in Fig.2, let $z_{d_0}^{J^*}$, $z_{d_{1+}}^{J^*}$, $z_{d_{1-}}^{J^*}$ represent the individual winding impedances connected to the PDNet, +120V wire and -120V wire along the single-phase SDNet, respectively. Let $I_{d_0}^{J^*}$, $I_{d_{1+}}^{J^*}$, $I_{d_{1-}}^{J^*}$ denote the currents flowing through $z_{d_0}^{J^*}$, $z_{d_{1+}}^{J^*}$, $z_{d_{1-}}^{J^*}$, $S_{d_0}^{J^*}$, $S_{d_{1+}}^{J^*}$, $S_{d_{1-}}^{J^*}$ denote the power flows flowing through $z_{d_0}^{J^*}$, $z_{d_{1+}}^{J^*}$, $z_{d_{1-}}^{J^*}$, respectively. We further define the current vector $\mathbf{I}_{d_1}^{J^*} \in \mathbb{C}^2$ and power flow vector $\mathbf{S}_{d_1}^{J^*} \in \mathbb{C}^2$, and the impedance matrix $\mathbf{Z}_d^{J^*} \in \mathbb{C}^{2 \times 2}$ for the center-tapped service transformer as follows:

$$\mathbf{I}_{d_1}^{J^*} = \begin{bmatrix} I_{d_{1+}}^{J^*} \\ I_{d_{1-}}^{J^*} \end{bmatrix}, \mathbf{S}_{d_1}^{J^*} = \mathbf{P}_{d_1}^{J^*} + j\mathbf{Q}_{d_1}^{J^*} = \begin{bmatrix} S_{d_{1+}}^{J^*} \\ S_{d_{1-}}^{J^*} \end{bmatrix}$$

$$\mathbf{Z}_d^{J^*} = \mathbf{R}_d^{J^*} + j\mathbf{X}_d^{J^*} = \begin{bmatrix} z_{d_{1+}}^{J^*} + z_{d_0}^{J^*} & -z_{d_0}^{J^*} \\ z_{d_0}^{J^*} & -(z_{d_{1-}}^{J^*} + z_{d_0}^{J^*}) \end{bmatrix}$$

Let \mathcal{N}^{J^*} denote the index set of non-head nodes in $SDNet(n_J, \phi_J)$, where $\mathcal{N}^{J^*} = \{n_1^{J^*}, \dots, n_{N^{J^*}}^{J^*}\}$, N^{J^*} is the number of non-head nodes in $SDNet(n_J, \phi_J)$. Note that $n_1^{J^*}$ is the low-voltage side of service transformer, which is usually connected to end users by triplex service lines. Each node $n_i^{J^*} \in \mathcal{N}^{J^*} \setminus \{n_1^{J^*}\}$ is electrically connected to a collection of customers $C(n_i^{J^*})$ by a phase- ϕ_J triplex service line that includes three wires, i.e., +120V wire, the ground wire, -120V

wire. Note that, as shown in Fig.2, any non-head node $n_i^{J^*}$ of $SDNet(n_J, \phi_J)$ consists of 2-wire points, i.e., +120V-wire point $n_{i+}^{J^*}$ and -120V-wire point $n_{i-}^{J^*}$. By definition of a radial network, each node located on a radial network can have at most one node that is an immediate predecessor. For each node $n_j^{J^*} \in \mathcal{N}^{J^*} \setminus \{n_1^{J^*}\}$, let $np(n_j^{J^*}) \in \mathcal{N}^{J^*}$ denote the node that immediately precedes node $n_j^{J^*}$ along the radial SDNet. Let $\mathcal{L}^{J^*} = \{(n_i^{J^*}, n_j^{J^*}) | n_i^{J^*} = np(n_j^{J^*}), n_j^{J^*} \in \mathcal{N}^{J^*} \setminus \{n_1^{J^*}\}\}$ denote the edge set of the radial network $SDNet(n_J, \phi_J)$, i.e., the collection of all triplex service lines for $SDNet(n_J, \phi_J)$.

For the head node $n_0^{J^*}$, let $V_0^{J^*}$ denote the voltage at node $n_0^{J^*}$, and $v_0^{J^*}$ denote the squared voltage magnitude of $V_0^{J^*}$. And let $\mathbf{V}_0^{J^*} \in \mathbb{C}^2$ denote the voltage vector for node $n_0^{J^*}$:

$$\mathbf{V}_0^{J^*} = \begin{bmatrix} V_0^{J^*} \\ V_0^{J^*} \end{bmatrix}$$

As depicted in Fig.2, for non-head node $n_i^{J^*} \in \mathcal{N}^{J^*}$, let $V_{i+}^{J^*}$ and $V_{i-}^{J^*}$ denote the voltage difference between its +120-wire point $n_{i+}^{J^*}$ and the ground wire and the voltage difference between the ground wire and its -120-wire point $n_{i-}^{J^*}$, $v_{i+}^{J^*}$ and $v_{i-}^{J^*}$ denote the squared voltage magnitude values of $V_{i+}^{J^*}$ and $V_{i-}^{J^*}$. Let $\mathbf{V}_i^{J^*} \in \mathbb{C}^2$ denote the voltage vector for node $n_i^{J^*} \in \mathcal{N}^{J^*}$:

$$\mathbf{V}_i^{J^*} = \begin{bmatrix} V_{i+}^{J^*} \\ V_{i-}^{J^*} \end{bmatrix}, \forall n_i^{J^*} \in \mathcal{N}^{J^*}$$

For node $n_i^{J^*} \in \mathcal{N}^{J^*} \setminus \{n_1^{J^*}\}$, let $s_{i+}^{J^*} = p_{i+}^{J^*} + jq_{i+}^{J^*}$, $s_{i-}^{J^*} = p_{i-}^{J^*} + jq_{i-}^{J^*}$, $s_{i+i-}^{J^*} = p_{i+i-}^{J^*} + jq_{i+i-}^{J^*}$ denote the 120V net load connected to +120V-wire point $n_{i+}^{J^*}$ and the ground wire, the 120V net load connected to the ground wire and -120V-wire point $n_{i-}^{J^*}$, the 240V load connected to $n_{i+}^{J^*}$ and $n_{i-}^{J^*}$, respectively. As depicted in Fig.2, let $I_{i+i-}^{J^*}$ denote the current flowing from $n_{i+}^{J^*}$ to $n_{i-}^{J^*}$ through the 240V load $s_{i+i-}^{J^*}$.

For each triplex service line segment $(n_i^{J^*}, n_j^{J^*}) \in \mathcal{L}^{J^*}$, let $I_{i+j+}^{J^*}$, $S_{i+j+}^{J^*} = P_{i+j+}^{J^*} + jQ_{i+j+}^{J^*}$ denote the current and power flow from +120V-wire point $n_{i+}^{J^*}$ to $n_{j+}^{J^*}$; let $I_{i-j-}^{J^*}$, $S_{i-j-}^{J^*} = P_{i-j-}^{J^*} + jQ_{i-j-}^{J^*}$ denote the current and power flow from -120V-wire point $n_{i-}^{J^*}$ to $n_{j-}^{J^*}$. Next, let $\mathbf{I}_{ij}^{J^*} \in \mathbb{C}^2$ and

$\mathbf{S}_{ij}^{J*} \in \mathbb{C}^2$ denote its current and power flow vectors as follows:

$$\mathbf{I}_{ij}^{J*} = \begin{bmatrix} I_{i+j+}^{J*} \\ I_{i-j-}^{J*} \end{bmatrix}, \forall (n_i^{J*}, n_j^{J*}) \in \mathcal{L}^{J*},$$

$$\mathbf{S}_{ij}^{J*} = \mathbf{P}_{ij}^{J*} + \mathbf{j}\mathbf{Q}_{ij}^{J*} = \begin{bmatrix} S_{i+j+}^{J*} \\ S_{i-j-}^{J*} \end{bmatrix}, \forall (n_i^{J*}, n_j^{J*}) \in \mathcal{L}^{J*}$$

Finally, for $(n_i^{J*}, n_j^{J*}) \in \mathcal{L}^{J*}$, let $\mathbf{Z}_{ij}^{J*} \in \mathbb{C}^{2 \times 2}$ denote its impedance matrix of triplex service line segment:

$$\mathbf{Z}_{ij}^{J*} = \mathbf{R}_{ij}^{J*} + \mathbf{j}\mathbf{X}_{ij}^{J*} = \begin{bmatrix} (z_{ij}^{++})^{J*}, (z_{ij}^{+-})^{J*} \\ -(z_{ij}^{+-})^{J*}, -(z_{ij}^{--})^{J*} \end{bmatrix}$$

where $(z_{ij}^{++})^{J*}, (z_{ij}^{--})^{J*}$ denote the self-impedances of +120V and -120V wires, and $(z_{ij}^{+-})^{J*}, (z_{ij}^{-+})^{J*}$ denote the mutual impedances between +120V and -120V wires.

C. Nonlinear SDNet Power Flow

According to [20], [21], service transformer power flow constraints are as follows:

$$\mathbf{V}_1^{J*} = \mathbf{V}_0^{J*} - \mathbf{Z}_d^{J*} \mathbf{I}_{d_1}^{J*} \quad (2a)$$

$$\mathbf{I}_{d_0}^{J*} = \mathbf{I}_{d_{1+}}^{J*} - \mathbf{I}_{d_{1-}}^{J*} \quad (2b)$$

Substituting $\mathbf{I}_{d_0}^{J*} = \mathbf{I}_{d_{1+}}^{J*} - \mathbf{I}_{d_{1-}}^{J*}$ into $\mathbf{S}_{d_0}^{J*} = \mathbf{V}_0^{J*} \overline{\mathbf{I}_{d_0}^{J*}}$, the power flow $\mathbf{S}_{d_0}^{J*}$ flowing through $z_{d_0}^{J*}$ can be represented as follows:

$$\mathbf{S}_{d_0}^{J*} = \mathbf{P}_{d_0}^{J*} + \mathbf{j}\mathbf{Q}_{d_0}^{J*} = \mathbf{V}_0^{J*} [\overline{\mathbf{I}_{d_{1+}}^{J*}} - \overline{\mathbf{I}_{d_{1-}}^{J*}}] \quad (3)$$

According to [20], [21], the Ohm's law for triplex service line segment $(n_i^{J*}, n_j^{J*}) \in \mathcal{L}^{J*}$ is expressed as follows:

$$\mathbf{V}_j^{J*} = \mathbf{V}_i^{J*} - \mathbf{Z}_{ij}^{J*} \mathbf{I}_{ij}^{J*}, \forall (n_i^{J*}, n_j^{J*}) \in \mathcal{L}^{J*} \quad (4)$$

For any 240V-load s_{i+-}^{J*} , it satisfies that:

$$s_{i+-}^{J*} = [\mathbf{V}_{i+}^{J*} + \mathbf{V}_{i-}^{J*}] \overline{\mathbf{I}_{i+-}^{J*}}, \forall n_i^{J*} \in \mathcal{N}^{J*} \setminus \{n_1^{J*}\} \quad (5)$$

IV. BRANCH FLOW MODEL FOR THE SDNET WITH SERVICE TRANSFORMERS

It is obvious that the nonlinear SDNet power flow model is non-convex, not suitable for performing OPF. For later convex optimization purposes, we first develop a branch flow model for the SDNet with service transformers, based on the nonlinear SDNet power flow model. Define slack variables $\boldsymbol{\ell}_d^{J*} \in \mathbb{C}^{2 \times 2}$, $\mathbf{W}_d^{J*} \in \mathbb{C}^{2 \times 2}$ as follows:

$$\boldsymbol{\ell}_d^{J*} = \mathbf{I}_{d_1}^{J*} [\mathbf{I}_{d_1}^{J*}]^H = \begin{bmatrix} \ell_{d_{1+}}^{J*}, \ell_{d_{1+-}}^{J*} \\ \ell_{d_{1+-}}^{J*}, \ell_{d_{1-}}^{J*} \end{bmatrix}$$

$$\mathbf{W}_d^{J*} = \mathbf{V}_0^{J*} [\mathbf{I}_{d_1}^{J*}]^H = \begin{bmatrix} S_{d_{0+}}^{J*}, S_{d_{0+-}}^{J*} \\ S_{d_{0+-}}^{J*}, S_{d_{0-}}^{J*} \end{bmatrix}$$

where:

$$\ell_{d_{1+}}^{J*} = I_{d_{1+}}^{J*} \overline{I_{d_{1+}}^{J*}} \quad (6a)$$

$$\ell_{d_{1-}}^{J*} = I_{d_{1-}}^{J*} \overline{I_{d_{1-}}^{J*}} \quad (6b)$$

$$\ell_{d_{1+-}}^{J*} = I_{d_{1+-}}^{J*} \overline{I_{d_{1+-}}^{J*}} \quad (6c)$$

$$S_{d_{0+}}^{J*} = P_{d_{0+}}^{J*} + \mathbf{j}Q_{d_{0+}}^{J*} = \mathbf{V}_0^{J*} \overline{I_{d_{1+}}^{J*}} \quad (6d)$$

$$S_{d_{0-}}^{J*} = P_{d_{0-}}^{J*} + \mathbf{j}Q_{d_{0-}}^{J*} = \mathbf{V}_0^{J*} \overline{I_{d_{1-}}^{J*}} \quad (6e)$$

We further introduce $\mathbf{U}_0^{J*} \in \mathbb{R}^{2 \times 2}$, and $\mathbf{v}_0^{J*} \in \mathbb{R}^2$ as follows:

$$\mathbf{U}_0^{J*} = \mathbf{V}_0^{J*} [\mathbf{V}_0^{J*}]^H = \begin{bmatrix} v_{0+}^{J*}, & v_{0+-}^{J*} \\ v_{0+-}^{J*}, & v_{0-}^{J*} \end{bmatrix}$$

$$\mathbf{v}_0^{J*} = \text{diag}(\mathbf{U}_0^{J*}) = \begin{bmatrix} v_{0+}^{J*} \\ v_{0-}^{J*} \end{bmatrix}$$

For any triplex service line segment $\forall (n_i^{J*}, n_j^{J*}) \in \mathcal{L}^{J*}$, we introduce slack variables $\boldsymbol{\ell}_{ij}^{J*} \in \mathbb{C}^{2 \times 2}$, $\mathbf{W}_{ij}^{J*} \in \mathbb{C}^{2 \times 2}$:

$$\boldsymbol{\ell}_{ij}^{J*} = \mathbf{I}_{ij}^{J*} [\mathbf{I}_{ij}^{J*}]^H = \begin{bmatrix} I_{i+j+}^{J*} \overline{I_{i+j+}^{J*}} & I_{i+j+}^{J*} \overline{I_{i-j-}^{J*}} \\ I_{i-j-}^{J*} \overline{I_{i+j+}^{J*}} & I_{i-j-}^{J*} \overline{I_{i-j-}^{J*}} \end{bmatrix} \quad (7a)$$

$$\mathbf{W}_{ij}^{J*} = \mathbf{V}_i^{J*} [\mathbf{I}_{ij}^{J*}]^H = \begin{bmatrix} V_{i+j+}^{J*} \overline{I_{i+j+}^{J*}} & V_{i+j+}^{J*} \overline{I_{i-j-}^{J*}} \\ V_{i-j-}^{J*} \overline{I_{i+j+}^{J*}} & V_{i-j-}^{J*} \overline{I_{i-j-}^{J*}} \end{bmatrix} = \begin{bmatrix} S_{i+j+}^{J*} & V_{i+j+}^{J*} \overline{I_{i-j-}^{J*}} \\ V_{i-j-}^{J*} \overline{I_{i+j+}^{J*}} & S_{i-j-}^{J*} \end{bmatrix} \quad (7b)$$

We also introduce $\mathbf{U}_i^{J*} \in \mathbb{C}^{2 \times 2}$, and $\mathbf{v}_i^{J*} \in \mathbb{R}^{2 \times 1}$ for $\forall (n_i^{J*}, n_j^{J*}) \in \mathcal{L}^{J*}$:

$$\mathbf{U}_i^{J*} = \mathbf{V}_i^{J*} [\mathbf{V}_i^{J*}]^H = \begin{bmatrix} V_{i+}^{J*} \overline{V_{i+}^{J*}} & V_{i+}^{J*} \overline{V_{i-}^{J*}} \\ V_{i-}^{J*} \overline{V_{i+}^{J*}} & V_{i-}^{J*} \overline{V_{i-}^{J*}} \end{bmatrix}$$

$$\mathbf{v}_i^{J*} = \text{diag}(\mathbf{U}_i^{J*}) = \begin{bmatrix} v_{i+}^{J*} \\ v_{i-}^{J*} \end{bmatrix}$$

With respect to (2a), multiply both sides by their Hermitian transposes, i.e., $[\mathbf{V}_1^{J*}]^H, [\mathbf{V}_0^{J*} - \mathbf{Z}_d^{J*} \mathbf{I}_d^{J*}]^H$, we have:

$$\mathbf{U}_1^{J*} = \mathbf{U}_0^{J*} - \mathbf{W}_d^{J*} [\mathbf{Z}_d^{J*}]^H - \mathbf{Z}_d^{J*} [\mathbf{W}_d^{J*}]^H + \mathbf{Z}_d^{J*} \boldsymbol{\ell}_d^{J*} [\mathbf{Z}_d^{J*}]^H \quad (8)$$

Apply $\text{diag}(\cdot)$ to (8), the squared voltage magnitude relationship for the service transformer is:

$$\mathbf{v}_1^{J*} = \mathbf{v}_0^{J*} - \text{diag}(\mathbf{W}_d^{J*} [\mathbf{Z}_d^{J*}]^H) - \text{diag}(\mathbf{Z}_d^{J*} [\mathbf{W}_d^{J*}]^H) + \text{diag}(\mathbf{Z}_d^{J*} \boldsymbol{\ell}_d^{J*} [\mathbf{Z}_d^{J*}]^H) \quad (9)$$

And (3) can be equivalently denoted by:

$$S_{d_0}^{J*} = [1, -1] \text{diag}(\mathbf{W}_d^{J*}) = S_{d_{0+}}^{J*} - S_{d_{0-}}^{J*} \quad (10)$$

With respect to (4), multiply both sides by their Hermitian transposes, i.e., $[\mathbf{V}_j^{J*}]^H, [\mathbf{V}_i^{J*} - \mathbf{Z}_{ij}^{J*} \mathbf{I}_{ij}^{J*}]^H$, then we have:

$$\begin{aligned} \mathbf{U}_j^{J*} &= [\mathbf{V}_i^{J*} - \mathbf{Z}_{ij}^{J*} \mathbf{I}_{ij}^{J*}] [\mathbf{V}_i^{J*} - \mathbf{Z}_{ij}^{J*} \mathbf{I}_{ij}^{J*}]^H \\ &= \mathbf{U}_i^{J*} - \mathbf{W}_{ij}^{J*} [\mathbf{Z}_{ij}^{J*}]^H - \mathbf{Z}_{ij}^{J*} [\mathbf{W}_{ij}^{J*}]^H \\ &\quad + \mathbf{Z}_{ij}^{J*} \boldsymbol{\ell}_{ij}^{J*} [\mathbf{Z}_{ij}^{J*}]^H, \forall (n_i^{J*}, n_j^{J*}) \in \mathcal{L}^{J*} \end{aligned} \quad (11)$$

Apply $\text{diag}(\cdot)$ to (11), the squared voltage magnitude relationship for triplex service lines is:

$$\begin{aligned} \mathbf{v}_j^{J*} &= \mathbf{v}_i^{J*} - \text{diag}(\mathbf{W}_{ij}^{J*} [\mathbf{Z}_{ij}^{J*}]^H) - \text{diag}(\mathbf{Z}_{ij}^{J*} [\mathbf{W}_{ij}^{J*}]^H) \\ &\quad + \text{diag}(\mathbf{Z}_{ij}^{J*} \boldsymbol{\ell}_{ij}^{J*} [\mathbf{Z}_{ij}^{J*}]^H), \forall (n_i^{J*}, n_j^{J*}) \in \mathcal{L}^{J*} \end{aligned} \quad (12)$$

Multiplying by the Hermitian transpose¹ of \mathbf{I}_{ij}^{J*} , i.e., $[\mathbf{I}_{ij}^{J*}]^H$, on both sides of (4), then we have:

$$\begin{aligned} \mathbf{V}_j^{J*} [\mathbf{I}_{ij}^{J*}]^H &= \mathbf{V}_i^{J*} [\mathbf{I}_{ij}^{J*}]^H - \mathbf{Z}_{ij}^{J*} \mathbf{I}_{ij}^{J*} [\mathbf{I}_{ij}^{J*}]^H \\ &= \mathbf{W}_{ij}^{J*} - \mathbf{Z}_{ij}^{J*} \boldsymbol{\ell}_{ij}^{J*}, \forall (n_i^{J*}, n_j^{J*}) \in \mathcal{L}^{J*} \end{aligned} \quad (13)$$

¹Hermitian transposes, indicated by superscript H , take the matrix transpose and then take the complex conjugate of each entry in the matrix.

Note that $\text{diag}(\mathbf{V}_j^{J*}[\mathbf{I}_{ij}^{J*}]^H)$ is the receiving-end power flow on triplex service line segment $(n_i^{J*}, n_j^{J*}) \in \mathcal{L}^{J*}$. Thus, the power balance for triplex service lines is expressed as follows:

$$\begin{aligned} \text{diag}(\mathbf{W}_{ij}^{J*} - \mathbf{Z}_{ij}^{J*} \ell_{ij}^{J*}) &= \sum_{(n_j^{J*}, n_k^{J*}) \in \mathcal{L}^{J*}} \text{diag}([\mathbf{W}_{jk}^{J*}]^H) \\ &+ \begin{bmatrix} s_{j+}^{J*} \\ s_{j-}^{J*} \end{bmatrix} + \begin{bmatrix} V_{j+}^{J*} \overline{I_{j+j-}^{J*}} \\ -V_{j-}^{J*} \overline{I_{j+j-}^{J*}} \end{bmatrix}, \forall n_j^{J*} \in \mathcal{N}^{J*} \setminus \{n_1^{J*}\} \end{aligned} \quad (14)$$

That is:

$$\begin{aligned} \mathbf{S}_{ij}^{J*} - \text{diag}(\mathbf{Z}_{ij}^{J*} \ell_{ij}^{J*}) &= \sum_{(n_j^{J*}, n_k^{J*}) \in \mathcal{L}^{J*}} \mathbf{S}_{jk}^{J*} + \begin{bmatrix} s_{j+}^{J*} \\ s_{j-}^{J*} \end{bmatrix} \\ &+ \begin{bmatrix} V_{j+}^{J*} \overline{I_{j+j-}^{J*}} \\ -V_{j-}^{J*} \overline{I_{j+j-}^{J*}} \end{bmatrix}, \forall n_j^{J*} \in \mathcal{N}^{J*} \setminus \{n_1^{J*}\} \end{aligned} \quad (15)$$

The power flow relationship between the service transformer and triplex service lines is:

$$\mathbf{S}_{d_1}^{J*} = \sum_{(n_1^{J*}, n_j^{J*}) \in \mathcal{L}^{J*}} \mathbf{S}_{1j}^{J*} \quad (16)$$

In short, SDNet branch flow constraints include service transformer constraints and triplex service line constraints. Service transformer constraints include:

- Slack variable constraints: (6)
- Voltage and power balance constraints for the single-phase center-tapped service transformer: (9),(10)

Triplex service line constraints include:

- The 240V-load constraints: (5)
- Slack variable constraints: (7)
- The voltage power balance constraints for triplex service lines: (12), (15)
- The power balance between the single-phase center-tapped service transformer and triplex service lines: (16)

V. CONVEX RELAXATION AND LINEARIZATION FOR SERVICE TRANSFORMER CONSTRAINTS

This section considers convex relaxation and linearization for service transformer constraints.

A. SOCP Relaxation for Service Transformers

The nonlinear equation (6) can be expressed as follows:

$$\text{real}(\ell_{d_{1+}}^{J*})^2 + \text{imag}(\ell_{d_{1+}}^{J*})^2 = \ell_{d_{1+}}^{J*} \ell_{d_{1-}}^{J*} \quad (17a)$$

$$\text{real}(S_{d_{0+}}^{J*})^2 + \text{imag}(S_{d_{0+}}^{J*})^2 = v_0^{J*} \ell_{d_{1+}}^{J*} \quad (17b)$$

$$\text{real}(S_{d_{0-}}^{J*})^2 + \text{imag}(S_{d_{0-}}^{J*})^2 = v_0^{J*} \ell_{d_{1-}}^{J*} \quad (17c)$$

$$\text{imag}(\ell_{d_{1+}}^{J*}) = 0, \text{imag}(\ell_{d_{1-}}^{J*}) = 0 \quad (17d)$$

The nonlinear equation (17) is still non-convex, we apply the SOCP relaxation to (17) as follows:

$$\text{real}(\ell_{d_{1+}}^{J*})^2 + \text{imag}(\ell_{d_{1+}}^{J*})^2 \leq \ell_{d_{1+}}^{J*} \ell_{d_{1-}}^{J*} \quad (18a)$$

$$\text{real}(S_{d_{0+}}^{J*})^2 + \text{imag}(S_{d_{0+}}^{J*})^2 \leq v_0^{J*} \ell_{d_{1+}}^{J*} \quad (18b)$$

$$\text{real}(S_{d_{0-}}^{J*})^2 + \text{imag}(S_{d_{0-}}^{J*})^2 \leq v_0^{J*} \ell_{d_{1-}}^{J*} \quad (18c)$$

$$\text{imag}(\ell_{d_{1+}}^{J*}) = 0, \text{imag}(\ell_{d_{1-}}^{J*}) = 0 \quad (18d)$$

Note that (18) can be rewritten as the standard second-order cone, which is convex:

$$\left\| \begin{bmatrix} 2\text{real}(\ell_{d_{1+}}^{J*}) \\ 2\text{imag}(\ell_{d_{1+}}^{J*}) \\ \ell_{d_{1+}}^{J*} - \ell_{d_{1-}}^{J*} \end{bmatrix} \right\|_2 \leq \left\| \ell_{d_{1+}}^{J*} + \ell_{d_{1-}}^{J*} \right\|_2 \quad (19a)$$

$$\left\| \begin{bmatrix} 2\text{real}(S_{d_{0+}}^{J*}) \\ 2\text{imag}(S_{d_{0+}}^{J*}) \\ v_0^{J*} - \ell_{d_{1+}}^{J*} \end{bmatrix} \right\|_2 \leq \left\| v_0^{J*} + \ell_{d_{1+}}^{J*} \right\|_2 \quad (19b)$$

$$\left\| \begin{bmatrix} 2\text{real}(S_{d_{0-}}^{J*}) \\ 2\text{imag}(S_{d_{0-}}^{J*}) \\ v_0^{J*} - \ell_{d_{1-}}^{J*} \end{bmatrix} \right\|_2 \leq \left\| v_0^{J*} + \ell_{d_{1-}}^{J*} \right\|_2 \quad (19c)$$

$$\text{imag}(\ell_{d_{1+}}^{J*}) = 0, \text{imag}(\ell_{d_{1-}}^{J*}) = 0 \quad (19d)$$

The SOCP-based service transformer constraints (SOCP-ST) are defined:

$$\text{SOCP-ST} = \{(9), (10), (18)\}$$

B. Linearization for Service Transformers

This part illustrates the linearization for non-convex service transformer constraints, which is based on [Assumption 1].

[Assumption 1]: The service transformer losses are relatively small compared to its power flows, i.e., $\mathbf{Z}_d^{J*} \ell_d^{J*} \ll \mathbf{W}_d^{J*}$.

Multiplying both sides of (2) by $(\mathbf{I}_{d_1}^{J*})^H$ and applying $\text{diag}(\cdot)$ to it, we have:

$$\begin{aligned} \text{diag}(\mathbf{V}_1^{J*} (\mathbf{I}_{d_1}^{J*})^H) &= \text{diag}(\mathbf{V}_0^{J*} (\mathbf{I}_{d_1}^{J*})^H) - \text{diag}(\mathbf{Z}_d^{J*} \ell_d^{J*}) \\ \mathbf{S}_{d_1}^{J*} &= \text{diag}(\mathbf{W}_d^{J*}) - \text{diag}(\mathbf{Z}_d^{J*} \ell_d^{J*}) \end{aligned} \quad (20)$$

Neglecting $\text{diag}(\mathbf{Z}_d^{J*} \ell_d^{J*})$ in (20) based on [Assumption 1], it follows that $\mathbf{S}_{d_1}^{J*} = \text{diag}(\mathbf{W}_d^{J*})$, i.e., :

$$\mathbf{P}_{d_1}^{J*} = \begin{bmatrix} P_{d_{0+}}^{J*} \\ P_{d_{0-}}^{J*} \end{bmatrix}, \mathbf{Q}_{d_1}^{J*} = \begin{bmatrix} Q_{d_{0+}}^{J*} \\ Q_{d_{0-}}^{J*} \end{bmatrix} \quad (21)$$

From [Assumption 1], we neglect $\text{diag}(\mathbf{Z}_{ij}^{J*} \ell_{ij}^{J*} [\mathbf{Z}_{ij}^{J*}]^H)$ in (9), then it follows:

$$\begin{aligned} \mathbf{v}_1^{J*} &= \mathbf{v}_0^{J*} - \text{diag}(\mathbf{W}_d^{J*} [\mathbf{Z}_d^{J*}]^H) - \text{diag}(\mathbf{Z}_d^{J*} [\mathbf{W}_d^{J*}]^H) \\ &= \mathbf{v}_0^{J*} - 2\mathbf{R}_d^{J*} \text{real}(\text{diag}(\mathbf{W}_d^{J*})) - 2\mathbf{X}_d^{J*} \text{imag}(\text{diag}(\mathbf{W}_d^{J*})) \\ &= \mathbf{v}_0^{J*} - 2\mathbf{R}_d^{J*} \begin{bmatrix} P_{d_{0+}}^{J*} \\ P_{d_{0-}}^{J*} \end{bmatrix} - 2\mathbf{X}_d^{J*} \begin{bmatrix} Q_{d_{0+}}^{J*} \\ Q_{d_{0-}}^{J*} \end{bmatrix} \end{aligned} \quad (22)$$

Substituting (21) into (22), we have:

$$\mathbf{v}_1^{J*} = \mathbf{v}_0^{J*} - 2\mathbf{R}_d^{J*} \mathbf{P}_{d_1}^{J*} - 2\mathbf{X}_d^{J*} \mathbf{Q}_{d_1}^{J*} \quad (23)$$

The linearized service transformer constraints (L-ST) are defined:

$$\text{L-ST} = \{(21), (23)\}$$

VI. LINEARIZATION FOR TRIPLEX SERVICE LINES

A. Linearized Triplex Service Line Power Flow

The linearized triplex service line power flow is proposed, based on the following [Assumption 2]:

- The voltage unbalances on each SDNet node $\forall n_i^{J*} \in \mathcal{N}^{J*}$ are not severe: $V_{i+}^{J*} \approx V_{i-}^{J*}$.
- The line losses are relatively small compared to the power flows, i.e., $\mathbf{Z}_{ij}^{J*} \ell_{ij}^{J*} \ll \mathbf{M}_{ij}^{J*}$.

From [Assumption 2], it indicates from (5) and (7) that:

$$V_{i+}^{J*} \overline{I_{i+}^{J*}} = V_{i-}^{J*} \overline{I_{i-}^{J*}} = \frac{S_{i+i-}^{J*}}{2}, \forall n_i^{J*} \in \mathcal{N}^{J*} \setminus \{n_1^{J*}\} \quad (24a)$$

$$\mathbf{W}_{ij}^{J*} = \begin{bmatrix} S_{i+j+}^{J*}, S_{i-j-}^{J*} \\ S_{i+j+}^{J*}, S_{i-j-}^{J*} \end{bmatrix}, \forall (n_i^{J*}, n_j^{J*}) \in \mathcal{L}^{J*} \quad (24b)$$

Neglecting $\text{diag}(\mathbf{Z}_{ij}^{J*} \ell_{ij}^{J*} [\mathbf{Z}_{ij}^{J*}]^H)$ in (12), and substituting (24b) into (12), then we have:

$$\mathbf{v}_j^{J*} = \mathbf{v}_i^{J*} - 2\mathbf{R}_{ij}^{J*} \mathbf{P}_{ij}^{J*} - 2\mathbf{X}_{ij}^{J*} \mathbf{Q}_{ij}^{J*}, \forall (n_i^{J*}, n_j^{J*}) \in \mathcal{L}^{J*} \quad (25)$$

Substituting (24a) into (15) and neglecting $\text{diag}(\mathbf{Z}_{ij}^{J*} \ell_{ij}^{J*})$ in (15) due to [Assumption 2], we have:

$$\begin{aligned} \mathbf{S}_{ij}^{J*} &= \sum_{(n_j^{J*}, n_k^{J*}) \in \mathcal{L}^{J*}} \mathbf{S}_{jk}^{J*} + \begin{bmatrix} s_{j+}^{J*} \\ s_{j-}^{J*} \end{bmatrix} \\ &+ \begin{bmatrix} \frac{s_{j+j-}^{J*}}{2} \\ -\frac{s_{j+j-}^{J*}}{2} \end{bmatrix}, \forall n_j^{J*} \in \mathcal{N}^{J*} \setminus \{n_1^{J*}\} \end{aligned} \quad (26)$$

That is:

$$\begin{aligned} \mathbf{P}_{ij}^{J*} &= \sum_{(n_j^{J*}, n_k^{J*}) \in \mathcal{L}^{J*}} \mathbf{P}_{jk}^{J*} + \begin{bmatrix} p_{j+}^{J*} \\ p_{j-}^{J*} \end{bmatrix} \\ &+ \begin{bmatrix} \frac{p_{j+j-}^{J*}}{2} \\ -\frac{p_{j+j-}^{J*}}{2} \end{bmatrix}, \forall n_j^{J*} \in \mathcal{N}^{J*} \setminus \{n_1^{J*}\} \end{aligned} \quad (27a)$$

$$\begin{aligned} \mathbf{Q}_{ij}^{J*} &= \sum_{(n_j^{J*}, n_k^{J*}) \in \mathcal{L}^{J*}} \mathbf{Q}_{jk}^{J*} + \begin{bmatrix} q_{j+}^{J*} \\ q_{j-}^{J*} \end{bmatrix} \\ &+ \begin{bmatrix} \frac{q_{j+j-}^{J*}}{2} \\ -\frac{q_{j+j-}^{J*}}{2} \end{bmatrix}, \forall n_j^{J*} \in \mathcal{N}^{J*} \setminus \{n_1^{J*}\} \end{aligned} \quad (27b)$$

Besides, (16) can be equivalently written as follows:

$$\mathbf{P}_{d_1}^{J*} = \sum_{(n_1^{J*}, n_j^{J*}) \in \mathcal{L}^{J*}} \mathbf{P}_{1j}^{J*} \quad (28a)$$

$$\mathbf{Q}_{d_1}^{J*} = \sum_{(n_1^{J*}, n_j^{J*}) \in \mathcal{L}^{J*}} \mathbf{Q}_{1j}^{J*} \quad (28b)$$

The linearized triplex service line constraints (L-TSL) are defined:

$$\text{L-TSL} = \{(25), (27), (28)\}$$

Case studies in Section VIII-A show that the L-TSL provides a good estimate of power flows and voltages. The L-TSL provides a linearized power flow model for SDNet.

B. Graph-Based Compact Power Flow Representation

Consider, first, the standard matrix representation $\overline{\mathbf{M}}^{J*} = [\mathbf{m}_1^{J*}, [\mathbf{M}^{J*}]^T]^T \in \mathbb{R}^{N^{J*} \times (N^{J*}-1)}$ for the incidence matrix of +120V-wire circuit in the SDNet. The rows of this matrix correspond to +120V-wire points, and the columns of this matrix correspond to +120V line segments. The entries of the matrix indicate, for each +120V-wire point and line segment, whether or not the +120-wire point is a ‘‘from’’ point or ‘‘to’’ node for this +120V line segment.

More precisely, $\overline{\mathbf{M}}^{J*}$ with an entry 1 for each ‘‘from’’ point and -1 for each ‘‘to’’ node takes the following form:

$$\overline{\mathbf{M}}^{J*} = \begin{bmatrix} \mathbb{J}(1, (np(n_2^{J*}), n_2^{J*})) & \dots & \mathbb{J}(1, (np(n_N^{J*}), n_N^{J*})) \\ \mathbb{J}(2, (np(n_2^{J*}), n_2^{J*})) & \dots & \mathbb{J}(2, (np(n_N^{J*}), n_N^{J*})) \\ \vdots & \vdots & \vdots \\ \mathbb{J}(N^{J*}, (np(n_2^{J*}), n_2^{J*})) & \dots & \mathbb{J}(N^{J*}, (np(n_N^{J*}), n_N^{J*})) \end{bmatrix} \quad (29)$$

where $\mathbb{J}(\cdot)$ is an indicator function defined as:

$$\mathbb{J}(i, (np(n_j^{J*}), n_j^{J*})) = \begin{cases} 1 & \text{if } n_i^{J*} = np(n_j^{J*}) \\ -1 & \text{if } n_i^{J*} = n_j^{J*} \\ 0 & \text{otherwise} \end{cases}$$

The first row $[\mathbf{m}_1^{J*}]^T$ of the matrix $\overline{\mathbf{M}}^{J*}$ represents the connection structure between +120V-wire point n_{1+}^{J*} and the line segments in \mathcal{L}^{J*} ; the remaining submatrix, denoted by \mathbf{M}^{J*} , represents the connection structure between the remaining +120V-wire points and +120V line segments. The tree topology of SDNet ensures that it is a connected graph, where \mathbf{M}^{J*} is a square matrix with full rank [25], and thus invertible.

Next, the incidence matrix $\overline{\mathbf{M}}^{J*}$ can be extended to the triplex line segments, consisting of +120V-wire circuit and -120V-wire circuit, in the SDNet. An extended incidence matrix $\overline{\mathbf{A}}^{J*} = [\mathbf{A}_1^{J*}, [\mathbf{A}^{J*}]^T]^T \in \mathbb{R}^{(2*N^{J*}) \times (2*N^{J*}-2)}$ for triplex service lines is constructed as follows:

$$\overline{\mathbf{A}}^{J*} = \overline{\mathbf{M}}^{J*} \otimes \mathbf{I}_2 \quad (30)$$

where

$$\begin{aligned} \mathbf{I}_2 &= 2 \times 2 \text{ identity matrix;} \\ \otimes &= \text{Kronecker product operation.} \end{aligned}$$

For $\forall n_i^{J*} \in \mathcal{N}^{J*} \setminus \{n_1^{J*}\}$, we define $\mathbf{p}_i^{J*} \in \mathbb{R}^2$ and $\mathbf{q}_i^{J*} \in \mathbb{R}^2$ as follows:

$$\mathbf{p}_i^{J*} = \begin{bmatrix} p_{i+}^{J*} \\ p_{i-}^{J*} \end{bmatrix} + \begin{bmatrix} \frac{p_{i+i-}^{J*}}{2} \\ -\frac{p_{i+i-}^{J*}}{2} \end{bmatrix} \quad (31a)$$

$$\mathbf{q}_i^{J*} = \begin{bmatrix} q_{i+}^{J*} \\ q_{i-}^{J*} \end{bmatrix} + \begin{bmatrix} \frac{q_{i+i-}^{J*}}{2} \\ -\frac{q_{i+i-}^{J*}}{2} \end{bmatrix} \quad (31b)$$

Define the following vectors:

$$\begin{aligned} \mathbf{v}^{J*} &= [[\mathbf{v}_2^{J*}]^T, \dots, [\mathbf{v}_N^{J*}]^T]^T \\ \mathbf{p}^{J*} &= [[\mathbf{p}_2^{J*}]^T, \dots, [\mathbf{p}_N^{J*}]^T]^T \\ \mathbf{q}^{J*} &= [[\mathbf{q}_2^{J*}]^T, \dots, [\mathbf{q}_N^{J*}]^T]^T \end{aligned}$$

²One simple example of incidence matrix construction for secondary distribution networks is given in Appendix A.

$$\begin{aligned} \mathbf{P}^{J*} &= [[\mathbf{P}_{np(2)2}^{J*}]^T, [\mathbf{P}_{np(3)3}^{J*}]^T, \dots, [\mathbf{P}_{np(N)N}^{J*}]^T]^T \\ \mathbf{Q}^{J*} &= [[\mathbf{Q}_{np(2)2}^{J*}]^T, [\mathbf{Q}_{np(3)3}^{J*}]^T, \dots, [\mathbf{Q}_{np(N)N}^{J*}]^T]^T \end{aligned}$$

where $\mathbf{P}_{np(j)j}^{J*}$, $\mathbf{Q}_{np(j)j}^{J*}$ denote the real and reactive power flow for the triplex service line $\ell_j^{J*} = (np(n_j^{J*}), n_j^{J*})$.

Resistances and reactances for triplex lines in \mathcal{L}^{J*} are compactly denoted by $2(N^{J*} - 1) \times 2(N^{J*} - 1)$ block diagonal matrices \mathbf{D}_r^{J*} and \mathbf{D}_x^{J*} as:

$$\begin{aligned} \mathbf{D}_r^{J*} &= \text{diag}(\mathbf{R}_{np(2)2}^{J*}, \mathbf{R}_{np(3)3}^{J*}, \dots, \mathbf{R}_{np(N)N}^{J*}) \\ \mathbf{D}_x^{J*} &= \text{diag}(\mathbf{X}_{np(2)2}^{J*}, \mathbf{X}_{np(3)3}^{J*}, \dots, \mathbf{X}_{np(N)N}^{J*}) \end{aligned}$$

where $\mathbf{R}_{np(j)j}^{J*}$, $\mathbf{X}_{np(j)j}^{J*}$ denote the resistance and reactance matrix for the triplex service line $\ell_j^{J*} = (np(n_j^{J*}), n_j^{J*})$.

In this case, (25) and (27) can be expressed as follows:

$$\mathbf{A}^{J*} \mathbf{P}^{J*} = -\mathbf{p}^{J*} \quad (32a)$$

$$\mathbf{A}^{J*} \mathbf{Q}^{J*} = -\mathbf{q}^{J*} \quad (32b)$$

$$[\mathbf{A}_1^{J*} \quad [\mathbf{A}^{J*}]^T] \begin{bmatrix} \mathbf{v}_1^{J*} \\ \mathbf{v}^{J*} \end{bmatrix} = 2(\mathbf{D}_r^{J*} \mathbf{P}^{J*} + \mathbf{D}_x^{J*} \mathbf{Q}^{J*}) \quad (32c)$$

The compact linearized triplex service line constraints (C-L-TSL) are defined:

$$\text{C-L-TSL} = \{(28), (31), (32)\}$$

[Remark]: It is worth mentioning that \mathbf{A}^{J*} is a square matrix with full rank and invertible since it satisfies $\mathbf{A}^{J*} = \mathbf{M}^{J*} \otimes \mathbf{I}_2$, where \mathbf{M}^{J*} is a square matrix with full rank and invertible.

VII. INTEGRATED PRIMARY-SECONDARY DISTRIBUTION NETWORK OPTIMAL POWER FLOW

The integrated primary-secondary distribution network OPF problem can be formulated as follows:

$$\min \text{Obj}(PDNet) + \text{Obj}(SDNet) \quad (33a)$$

$$s.t. \text{ PDNet constraints} \quad (33b)$$

$$\text{SDNet constraints} \quad (33c)$$

$$\text{PDNet and SDNet coupling constraints} \quad (33d)$$

For PDNet constraints, they have been widely investigated in existing works. The linearized PDNet power flow (1) [13] or the SDP-based PDNet power flow [12], [13] can both be applied to express PDNet constraints, which can be expressed as follows:

$$\text{Linearized or SDP-based PDNet power flow} \quad (34a)$$

$$\mathbf{v}_I^{min} \leq \mathbf{v}_I \leq \mathbf{v}_I^{max}, \forall n_I \in \mathcal{N} \quad (34b)$$

And SDNet constraints can be expressed as follows:

$$\text{SOCP-ST or L-ST}, \forall J* \in \mathcal{J} \quad (35a)$$

$$\text{L-TSL}, \forall J* \in \mathcal{J} \quad (35b)$$

$$\mathbf{v}_i^{min} \leq \mathbf{v}_i^{J*} \leq \mathbf{v}_i^{max}, \forall n_i^{J*} \in \mathcal{N}^{J*}, \forall J* \in \mathcal{J} \quad (35c)$$

$$\mathbf{p}_i^{J*} = \mathbf{p}_{i,l}^{J*} - \mathbf{p}_{i,d}^{J*}, \forall n_i^{J*} \in \mathcal{N}^{J*}, \forall J* \in \mathcal{J} \quad (35d)$$

$$\mathbf{q}_i^{J*} = \mathbf{q}_{i,l}^{J*} - \mathbf{q}_{i,d}^{J*}, \forall n_i^{J*} \in \mathcal{N}^{J*}, \forall J* \in \mathcal{J} \quad (35e)$$

$$\underline{\mathbf{p}}_{i+}^{J*} \leq \mathbf{p}_{i+}^{J*} \leq \bar{\mathbf{p}}_{i+}^{J*}, \underline{\mathbf{p}}_{i-}^{J*} \leq \mathbf{p}_{i-}^{J*} \leq \bar{\mathbf{p}}_{i-}^{J*},$$

$$\underline{\mathbf{p}}_{i+i-}^{J*} \leq \mathbf{p}_{i+i-}^{J*} \leq \bar{\mathbf{p}}_{i+i-}^{J*}, \forall n_i^{J*} \in \mathcal{N}^{J*}, \forall J* \in \mathcal{J} \quad (35f)$$

$$\underline{\mathbf{q}}_{i+}^{J*} \leq \mathbf{q}_{i+}^{J*} \leq \bar{\mathbf{q}}_{i+}^{J*}, \underline{\mathbf{q}}_{i-}^{J*} \leq \mathbf{q}_{i-}^{J*} \leq \bar{\mathbf{q}}_{i-}^{J*},$$

$$\underline{\mathbf{q}}_{i+i-}^{J*} \leq \mathbf{q}_{i+i-}^{J*} \leq \bar{\mathbf{q}}_{i+i-}^{J*}, \forall n_i^{J*} \in \mathcal{N}^{J*}, \forall J* \in \mathcal{J} \quad (35g)$$

where \mathcal{J} denotes the node set that includes all coupling nodes between the PDNet and SDNets. (35a) is service transformer constraints, (35b) is triplex service line constraints, (35c) is SDNet voltage limits, (35d)-(35e) denote the values of net loads are equal to the values of loads minus the values of DERs, e.g., distributed generators, (35f)-(35g) denote the power limits for net load consumption.

For the coupling constraints between the PDNet and any $SDNet(n_J, \phi_J)$, they are expressed as follows:

$$v_0^{J*} = v_J^{\phi_J}, \forall J* \in \mathcal{J} \quad (36a)$$

$$P_{d_0}^{J*} + jQ_{d_0}^{J*} = p_J^{\phi_J} + jq_J^{\phi_J}, \forall J* \in \mathcal{J} \quad (36b)$$

The equation (36a) indicates that the squared voltage magnitude v_0^{J*} of node n_0^{J*} in the $SDNet(n_J, \phi_J)$ is the same as the phase- ϕ_J squared voltage magnitude $v_J^{\phi_J}$ of bus n_J in the PDNet. The equation (36b) indicates that the real and reactive power flows, $P_{d_0}^{J*}$ and $Q_{d_0}^{J*}$, flowing through $z_{d_0}^{J*}$ are the same as the phase- ϕ_J real and reactive power loads of bus n_J in the PDNet.

VIII. CASE STUDY

In this section, we highlight the great significance of including SDNets in power flow analysis, and further evaluate the effectiveness and accuracy of our proposed models.

A. Accuracy of L-ST and L-TSL

To test the accuracy of L-ST and L-TSL, we consider the following three models:

- Model 1 (PDNet model): This model only considers the PDNet model, where the loads and DERs in SDNets are aggregated at the PDNet bus.
- Model 2 (Accurate primary-secondary distribution networks): This model considers both PDNet and SDNet models, where SDNets are modeled by means of OpenDSS [26] to consider the nonlinear SDNets power flows.
- Model 3 (Simplified primary-secondary distribution networks): This model utilizes the L-ST and L-TSL to model SDNets.

Specifically, Model 1 only considers the PDNet without SDNets. Model 2 considers both the PDNet and SDNets, and performs the nonlinear power flow in primary-secondary distribution networks, which can be regarded as the benchmark. Model 3 also includes the PDNet and SDNets, but it performs the linearized PDNet power flow in [13] and the linearized SDNet power flow by our proposed L-ST and L-TSL.

We first compare Models 1, 2 and 3 in two different test systems, one is a modified 12-bus PDNet system with 12 SDNets [27]-[28], as shown in Fig. 3, another one is a real utility primary-secondary distribution network in the U.S., as shown

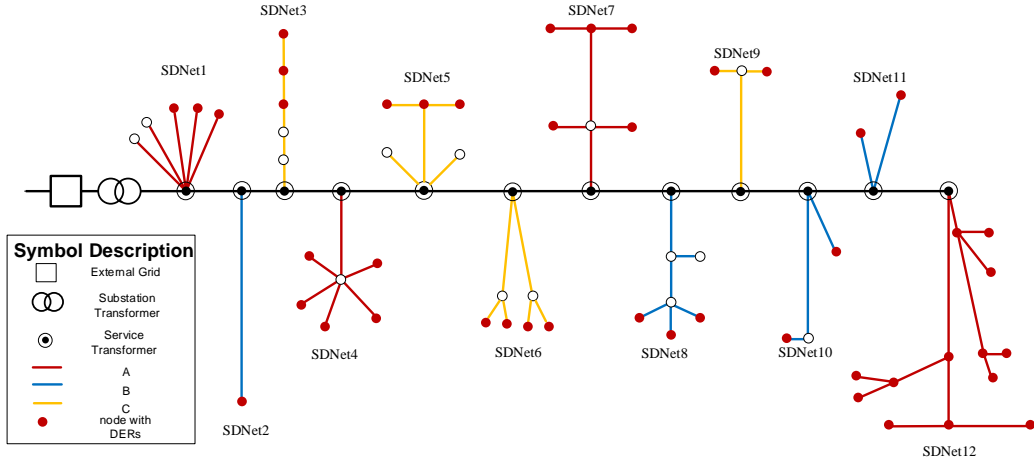


Fig. 3. A modified 12-bus PDNet system with 12 SDNets

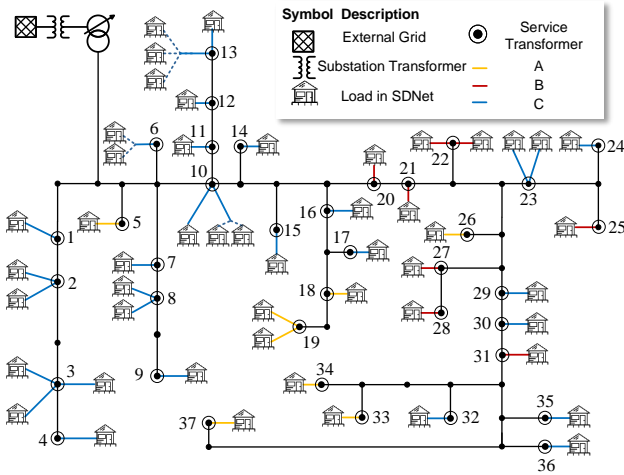


Fig. 4. A real utility primary-secondary distribution network in U.S.

in Fig. 4. Fig. 5 and Fig. 6 show voltage distributions calculated by Models 1, 2, and 3 in the above two test systems, respectively. As shown in Fig. 5 and Fig. 6, Model 1 only reflects voltage distributions across the PDNets of two test systems, depicted by the red dotted line, due to the lack of SDNets. Instead, Models 2 and 3 exhibit the capability of depicting voltage distributions across each SDNet of two test systems, where the voltage distributions for +120V and -120V circuits of SDNet are represented by the blue and orange markers, and the SDNet voltage distributions of Model 3 closely track Model 2. In addition, Models 2 and 3 can detect the under-voltage violations of SDNet 12 in the modified 12-bus PDNet system, shown in Fig.5, and SDNets 2 and 19 in the real utility primary-secondary distribution network, shown in Fig.6, but Model 1 fails to reflect the voltage violations in SDNets of test systems. The safe operation of PDNet cannot guarantee the safe operation of SDNet.

Next, we consider a series of different load conditions, and use Model 2 to calculate the real power flows and voltage magnitudes as the benchmark. Also, we utilize Models 1 and 3 to

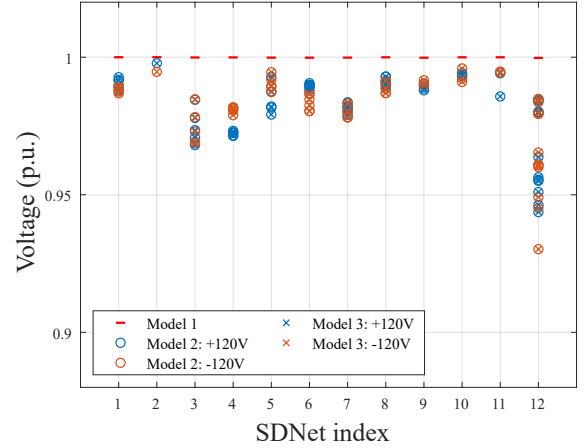


Fig. 5. Voltage distributions calculated by Models 1, 2, and 3 in the modified 12-bus PDNet with 12 SDNets.

TABLE I
ACCURACY COMPARISON: A MODIFIED 12-BUS PDNET SYSTEM WITH 12 SDNETS

	P (%)	V_{pri} (p.u.)	V_{sec} (p.u.)
Model1	1.88	2.63e-06	-
Model3	1.89	2.55e-06	5.69e-04

approximately estimate the power flows and voltage magnitudes, and compare their differences with Model 2, where the average errors of the power exchange at the substation transformer of PDNet, the PDNet voltage magnitudes, and the SDNet voltage magnitudes, i.e., $P(\%)$, $V_{pri}(p.u.)$, $V_{sec}(p.u.)$, are selected as the metrics to evaluate the performance of Mod-

TABLE II
ACCURACY COMPARISON: A REAL UTILITY PRIMARY-SECONDARY DISTRIBUTION NETWORK

	P (%)	V_{pri} (p.u.)	V_{sec} (p.u.)
Model1	2.02	2.09e-5	-
Model3	2.47	2.21e-5	1.1e-3

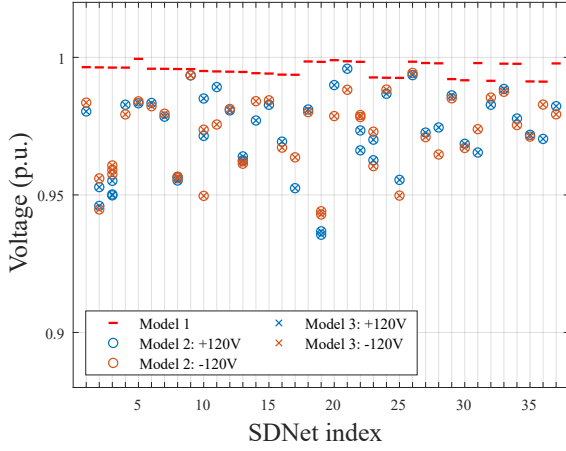


Fig. 6. Voltage distributions calculated by Models 1, 2, and 3 in the real utility primary-secondary distribution network in U.S.

els 1 and 3 compared to Model 2. As shown in Tables I-II, the errors of P(%) for Models 1 and 3 are around 2% compared to Model 2 for both test systems. In addition, Model 1 cannot reflect the SDNet operations, which does not provide information for SDNet voltage magnitude errors V_{sec} . Instead, SDNet voltage magnitude errors V_{sec} are very small of Model 3 compared to Model 2 in both test systems, which are $5.69e-04$ and $1.1e-3$, respectively. The results indicate our proposed L-ST and L-TSL can provide a good estimate of real SDNet voltage magnitudes.

B. Integrated Primary-Secondary Distribution Network OPF

This subsection considers a primary-secondary distribution network OPF problem, where the optimization goal is assumed to minimize SDNet power losses by dispatching DERs distributed across SDNets. And the linearized PDNet power flow, SOCP-ST and L-TSL are utilized in (34)-(35). Taking the modified 12-bus PDNet system with 12 SDNets as one example, Fig.7 depicts the aggregate load consumption for each SDNet. In addition, there are flexible DERs and loads, connected to SDNets shown in Fig.3 and Fig.4. For these DERs distributed across SDNets, it is assumed that each DER can absorb/generate at most 1 kW real power and 1 kVar reactive power for the +120V circuit, 2 kW real power and 2 kVar reactive power for the -120V circuit, and 2 kW real power and 2 kVar reactive power for the 240V circuit.

Taking SDNets 1 and 5 as examples, the OPF-based voltage distributions, determined by this primary-secondary distribution system OPF, and the real voltage distributions, determined by inputting the optimal DER outputs into OpenDSS, are depicted in Fig.8 and Fig.9. There are not many differences between the OPF-based and real voltage distributions. This proposed integrated primary-secondary distribution network OPF effectively exhibits the capability of reflecting the voltage distributions and controlling DERs in SDNets.

IX. CONCLUSIONS

This paper proposes an optimal power flow for integrated primary-secondary distribution networks with service trans-

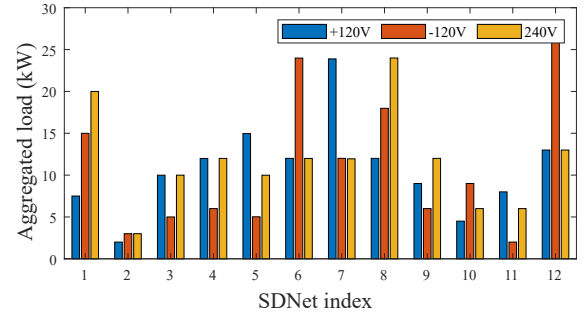


Fig. 7. Aggregate load consumption for each SDNet in the modified 12-bus PDNet with 12 SDNets

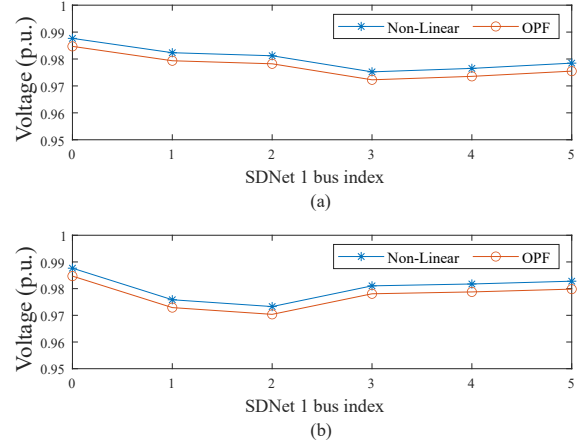


Fig. 8. Voltage magnitudes of SDNet 1: (a) +120V line. (b): -120V line.

formers. Instead of neglecting SDNets with service transformers, we model SDNets, including service transformers and triplex service lines, in the integrated primary-secondary distribution network OPF. To be more specific, the SOCP relaxation and linearization for the service transformer power flow, i.e., SOCP-ST and L-ST, are proposed, and the linearized power flow for triplex service lines, i.e., L-TSL/ C-L-TSL, is developed. Numerical studies are performed to show the effectiveness and superiority of our proposed models.

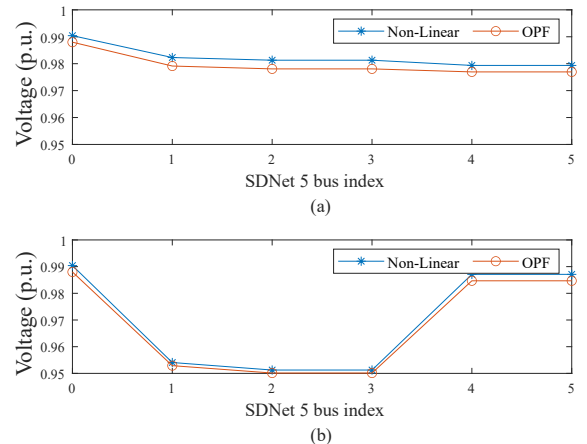


Fig. 9. Voltage magnitudes of SDNet 5: (a) +120V line. (b): -120V line.

One remaining challenge is the observable information of SDNet models. For example, current sensing technologies only provide aggregate power demands at these customer locations, but do not independently provide the detailed information of loads at 120V and 240V levels. In the future, we will strive to resolve this disaggregation challenge. In addition, we will explore different power system applications in integrated primary-secondary distribution networks by means of our proposed integrated primary-secondary distribution network OPF.

APPENDIX A

Incidence Matrix Construction for Secondary Distribution Networks:

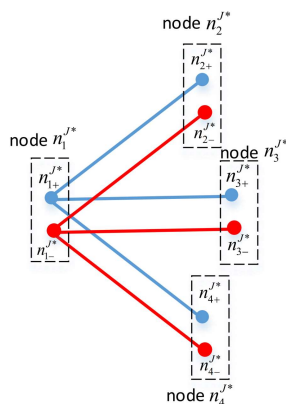


Fig. 10. Secondary distribution network illustration

To illustrate the construction of the incidence matrices \bar{M}^{J*} and \bar{A}^{J*} introduced in Section VI for triplex service lines in SDNets, consider Fig.10. This SDNet consists of 3 triplex service lines, where $\mathcal{L}^{J*} = \{(n_1^{J*}, n_2^{J*}), (n_1^{J*}, n_3^{J*}), (n_1^{J*}, n_4^{J*})\}$.

Then, the incidence matrix \bar{M}^{J*} for +120V-wire circuit in this SDNet takes the following form:

$$\bar{M}^{J*} = \begin{bmatrix} 1 & 1 & 1 \\ -1 & 0 & 0 \\ 0 & -1 & 0 \\ 0 & 0 & -1 \end{bmatrix} \quad (37)$$

Next, the incidence matrix $\bar{A}^{J*} = \bar{M}^{J*} \otimes \mathbf{I}_2$ for the triplex service lines then takes the following form:

$$\bar{A}^{J*} = \begin{bmatrix} 1 & 0 & 1 & 0 & 1 & 0 \\ 0 & 1 & 0 & 1 & 0 & 1 \\ -1 & 0 & 0 & 0 & 0 & 0 \\ 0 & -1 & 0 & 0 & 0 & 0 \\ 0 & 0 & -1 & 0 & 0 & 0 \\ 0 & 0 & 0 & -1 & 0 & 0 \\ 0 & 0 & 0 & 0 & -1 & 0 \\ 0 & 0 & 0 & 0 & 0 & -1 \end{bmatrix} \quad (38)$$

REFERENCES

- [1] R.A. Jabr, "Radial distribution load flow using conic programming," *IEEE Trans. Power Syst.*, vol. 21, no. 3, pp. 1458-1459, Aug. 2006.
- [2] M. Farivar and S.H. Low, "Branch flow model: relaxations and convexification," *IEEE Trans. Power Syst.*, vol. 28, no. 3, pp. 2554-2564, 2013.
- [3] X. Bai, H. Wei, K. Fujisawa, and Y. Wang, "Semidefinite programming for optimal power flow problems," *Int. J. Elect. Power Energy Syst.*, vol. 30, no. 6-7, pp. 383-392, 2008.
- [4] J. Lavaei and S.H. Low, "Zero duality gap in optimal power flow problem," *IEEE Trans. Power Syst.*, vol. 27, no. 1, pp. 92-107, Feb. 2012.
- [5] M.S. Andersen, A. Hansson, and L. Vandenberghe, "Reduced-complexity semidefinite relaxations of optimal power flow problems," *IEEE Trans. Power Syst.*, vol. 29, no. 4, pp. 1855-1863, Jul. 2014.
- [6] S. Bose, S.H. Low, T. Teeraratkul, and B. Hassibi, "Equivalent relaxations of optimal power flow," *IEEE Trans. Autom. Control*, vol. 60, no. 3, pp. 729-742, Mar. 2015.
- [7] S.V. Dhople, S.S. Guggilam, and Y.C. Chen, "Linear approximations to ac power flow in rectangular coordinates," in *Allerton Conference on Communication, Control, and Computing*, Sept. 2015, pp. 211-217.
- [8] M.E. Baran and F.F. Wu, "Network reconfiguration in distribution system for loss reduction and load balancing," *IEEE Trans. Power Del.*, vol. 4, no. 2, pp. 1401-1407, Apr. 1989.
- [9] M.E. Baran and F.F. Wu, "Optimal sizing of capacitors placed on a radial distribution system," *IEEE Trans. Power Del.*, vol. 4, no. 1, pp. 735-743, Jan. 1989.
- [10] M. Farivar, L. Chen, and S. Low, "Equilibrium and dynamics of local voltage control in distribution systems," in *Proc. IEEE 52nd Conf. Decision and Control (CDC)*, Dec. 2013, pp. 4329-4334.
- [11] V. Kekatos, L. Zhang, G. B. Giannakis, and R. Baldick, "Fast localized voltage regulation in single-phase distribution grids," in *Proc. IEEE Int. Conf. Smart Grid Commun.*, Miami, FL, USA, Nov. 2015.
- [12] E. Dall'Anese, H. Zhu, and G.B. Giannakis, "Distributed optimal power flow for smart microgrids," *IEEE Trans. Smart Grid*, vol. 4, no. 3, pp. 1464-1475, Sep. 2013.
- [13] L. Gan and S.H. Low, "Convex relaxations and linear approximation for optimal power flow in multiphase radial network," in *18th Power Systems Computation Conference (PSCC)*, 2014.
- [14] A. Garces, "A linear three-phase load flow for power distribution systems," *IEEE Trans. Power Syst.*, vol. 31, no. 1, pp. 827-828, Jan. 2016.
- [15] B.A. Robbins and A.D. Domínguez-García, "Optimal reactive power dispatch for voltage regulation in unbalanced distribution systems," *IEEE Trans. Power Syst.*, vol. 31, no. 4, pp. 2903-2913, Jul. 2016.
- [16] R. Cheng, Z. Wang and Y. Guo, "An online feedback-based linearized power flow model for unbalanced distribution networks," *IEEE Trans. Power Syst.*, vol. 37, no. 5, pp. 3552-3565, Sept. 2022.
- [17] B. V. Rao, F. Kupzog, and M. Kozek, "Three-phase unbalanced optimal power flow using holomorphic embedding load flow method," *Sustainability*, vol. 11, no. 6, pp. 1774, 2019, MDPI.
- [18] J. S. Giraldo, P. P. Vergara, J. C. López, P. H. Nguyen, and N. G. Paterakis, "A Linear AC-OPF Formulation for Unbalanced Distribution Networks," *IEEE Transactions on Industry Applications*, vol. 57, no. 5, pp. 4462-4472, 2021, doi: 10.1109/TIA.2021.3085799.
- [19] S. Claeys, F. Geth, and G. Deconinck, "Optimal power flow in four-wire distribution networks: formulation and benchmarking," *Electric Power Systems Research*, vol. 213, p. 108522, 2022, Elsevier.
- [20] W. H. Kersting, "Center-Tapped transformer and 120-/240-V secondary models," *IEEE Transactions on Industry Applications*, vol. 45, no. 2, pp. 575-581, 2009.
- [21] W. H. Kersting, *Distribution System Modeling and Analysis*, 2nd ed. Boca Raton, FL: CRC Press, 2007.
- [22] R. Panigrahi, S. K. Mishra, S. C. Srivastava, A. K. Srivastava and N. N. Schulz, "Grid integration of small-scale photovoltaic systems in secondary distribution network—a review," *IEEE Transactions on Industry Applications*, vol. 56, no. 3, pp. 3178-3195, May-June 2020.
- [23] A.R. Malekpour, A.Pahwa and B. Natarajan, "Hierarchical architecture for integration of rooftop PV in smart distribution systems," *IEEE Trans. Smart Grid*, vol. 9, no. 3, pp. 2019-2029, May 2018.
- [24] Q. Zhang, Y. Guo, Z. Wang and F. Bu, "Distributed Optimal Conservation Voltage Reduction in Integrated Primary-Secondary Distribution Systems," *IEEE Trans. Smart Grid*, vol. 12, no. 5, pp. 3889-3900, Sept. 2021.
- [25] D. B. West, *Introduction to Graph Theory*, 2nd ed. Upper Saddle River, NJ, USA: Prentice Hall, 2001.
- [26] R. C. Dugan and T. E. McDermott, "An open source platform for collaborating on smart grid research," in *Proc. IEEE Power Energy Soc. Gen. Meeting*, Jul. 2011, pp. 1-7.
- [27] "Secondary Test Circuit Modified", [Online] Available: https://sourceforge.net/p/electricdss/code/HEAD/tree/trunk/Version8/Distrib/IEEETestCases/SecondaryTestCircuit_modified/
- [28] "IEEE-TIA-LV Model ", [Online] Available: <https://sourceforge.net/p/electricdss/code/HEAD/tree/trunk/Version8/Distrib/Examples/Scripts/IEEE-TIA-LV%20Model/>